Energy 167 (2019) 1266–1277

Contents lists available at ScienceDirect

Energy

journal homepage: www.elsevier.com/locate/energy

A two-layer model for dynamic pricing of electricity and optimal charging of electric vehicles under price spikes

Vignesh Subramanian*, Tapas K. Das

Department of Industrial and Management Systems Engineering, University of South Florida, Tampa, FL, 33620, USA

ARTICLE INFO

Article history:
Received 23 August 2018
Received in revised form
10 October 2018
Accepted 27 October 2018
Available online 2 November 2018

Keywords:
Dynamic pricing
Electric vehicles
Demand response
Mathematical program with equilibrium constraints
Robust optimization

ABSTRACT

Pilot projects in power networks conducted across continents have established the benefits of dynamic pricing by inducing increased demand response. However, a key hurdle in the growth of demand response is the lack of widespread availability of advanced metering infrastructure, which has stymied the adoption of dynamic pricing. We believe that this hurdle will be partially addressed by the growth of electric vehicles (EVs), as smart and connected EV parking lots will be a provider of demand response. We develop a two-layer optimization model that simultaneously determines dynamic pricing policy for the system operator and demand response strategies for the EV parking lots. The model minimizes the cost to consumers, while ensuring the system operator's revenue neutral status and addressing real-time price uncertainties. A variant of the 5-bus PJM network is used to demonstrate model implementation. Numerical results show that for a low to moderate price spike scenario, dynamic pricing with demand response from EVs alone can lower the daily average consumer cost of 1.42% compared to the cost of flat pricing. A cost reduction of 6.5% is achieved when price spikes are relatively high. Computational challenges of implementing our model for real networks are discussed in the concluding remarks.

1. Introduction

It was recommended early in the new millennium that power networks will benefit significantly from dynamic pricing and demand response [1]. Some of the recent review papers that futher emphasize this are [2–4]. Till date, dynamic pricing policies have remained limited to variants of time of use (TOU), critical peak pricing (CPP), and ex-post real time pricing (RTP). The lack of availability of a pure form of dynamic pricing, where binding prices are offered to consumers just ahead of power usage, has limited the incentives for demand response to grow. As a result, historically, hourly demand for electricity has remained highly uneven and has continued to cause significant price spikes. It is estimated that networks maintain 10–15% of the average demand as reserve capacity to deal with uneven load distribution. Also, 10% of the cost of electricity is spent in 1% of the operating times due to price spikes [5,6]. For example, in the month of May 2018, the price of electricity in the ERCOT market in the U.S. spiked from the average level of $25-$60/MWh to $750-$1600/MWh. During the same period the price in the NYISO market in the U.S. experienced price fluctuations in the range of -$600/MWh to $1000/MWh [7]. The woes of power networks may be exacerbated in coming years with the explosion of EVs and resulting increase in energy demand as well as change in daily load patterns. It is estimated that the number of EVs will grow to 7.3 million by 2023 in the U.S. [8]. Considering an average battery capacity of 70 kWh, charging of these batteries even once a day may consume up to an additional 500,000 MWh. Unless managed well, this consumption growth could significantly alter the current daily load profile and further increase price spikes. We recognize, however, that the growth of EVs will also bring an unique opportunity for increased demand response. Large number of EVs will be parked in smart, connected, and aggregator managed parking lots. While parked, these EVs will be charged optimally and thus will likely shift EV demand to off-peak periods and reduce stress on the network.

In this paper we present a two-layer optimization model to develop policies for implementing pure dynamic pricing of electricity and demand response using EVs. The top-layer of our model addresses the day-ahead (DA) market operations using a two-stage stochastic model that considers different demand patterns and uncertain real-time (RT) prices. The RT market operations, using DA solutions as an input, are considered in the bottom-layer and are

* Corresponding author.
E-mail address: vigneshs@mail.usf.edu (V. Subramanian).

https://doi.org/10.1016/j.energy.2018.10.171
0360-5442/

formulated as a bilevel model which is solved for each hour of the day, just before dispatch. The upper-level of the bilevel model solves for dynamic prices and the lower-level determines the demand response action (optimal charging).

The important features of our two-layer model are the following: 1) the top-layer model considers power network configurations including congestion, 2) the bilevel model uses a robust optimization framework to accommodate RT price uncertainties, 3) the upper-level of the bilevel model uses a specific constraint to manage revenue neutrality of the system operator (SO), 4) a mixture of two probability distributions is used to generate price spikes, their magnitude and time of occurrence and 5) a granular parking lot model with a large volume of EVs comprising different makes, models, battery capacities, and charging needs. As regards solution of the model, we first reformulate the bilevel model into a single level mathematical program with equilibrium constraints (MPEC) model. We then linearize the MPEC model using the strong duality principle. The resulting optimization model is a single level mixed integer linear programming (MILP), which is solved using a conventional approach. In the rest of this section, a short review of literature on dynamic pricing and demand response is presented.

A pure form of dynamic pricing, where binding prices are declared just ahead of consumption in small intervals (say, an hour or less), is often referred to in the literature as real time pricing, RTP. However, the nomenclature of dynamic pricing and RTP is used widely in the literature to include many other forms of time varying pricing strategies. Such strategies include: block rate tariffs, seasonal tariffs, TOU, superpeak TOU, CPP, variable peak pricing (VPP), and RTP; see Ref. [2] for definitions of these pricing schemes. Henceforth, in this paper, we will only consider the pure form of dynamic pricing that offers binding prices ahead of consumption. Implementation of this dynamic pricing requires availability of advanced metering infrastructure (AMI). Literature shows that availability of smart technology increases price elasticity and grid efficiency [9–11]. Beneficial impacts of dynamic pricing have been explored through many pilot projects in recent years. The survey presented in Ref. [12] examined seventy-four dynamic pricing experiments across three continents during the last decade. The results show that increase in price peaks offers better benefits of load balancing from dynamic pricing. It is shown in Ref. [13] that dynamic pricing can achieve a peak demand reduction of 10–14%, customer cost reduction of 2–5%, and a social welfare increase by $141-$403 million in a year. A study conducted in California [14] found that most consumers will benefit from dynamic pricing, and also that low income consumers will not be impacted negatively, a concern that was expressed earlier. Even with well documented benefits of dynamic pricing, its implementation in power network still remains a challenge. This is due to the lack of adoption of AMI, and, to our knowledge, need for models that can yield appropriate dynamic pricing strategies for networks affected by price volatility.

Though broad availability of AMI for consumers to engage in demand response remains a capital investment challenge, a significant number of papers have been presented to the literature that address demand response by residential thermostatic loads and distributed generation. In Ref. [15], a two-stage stochastic optimization model is developed for the aggregators to optimally control flexible thermostatic loads (e.g., water and space heaters) and buy back from prosumers' storage to trade in spot markets to minimize overall cost. The same authors in Ref. [16] considered a multi-stage stochastic modeling approach for the aggregators to minimize prosumers' cost by bidding sequentially in the option market, DA market, and near RT market. In the model presented in Ref. [17], the aggregators first determine the DA quantity considering EV, thermostatic loads, shiftable load, and renewable generation. Thereafter, a model predictive control approach is used to adjust the flexible loads to minimize the net cost of buying and selling energy in the RT market. It is claimed that this strategy reduces the net cost of aggregators by 14% compared with operation with no DR. A bi-objective optimization model in Ref. [18] develops a tradeoff between user comfort and cost of energy consumption in smart buildings. It is shown in Ref. [19] that a 17% energy cost saving can be attained through DR in residential microgrids equipped with photovoltaic systems, flexible loads, and electric vehicles. The savings can be further increased by 6% if battery storage is available. A recent paper in Ref. [20] obtains simultaneous strategies for dynamic pricing by SO and demand response by load aggregators using a data driven iterative learning approach.

We believe that the impending growth of EVs will bring new opportunities for power networks as the aggregator managed EV parking lots will supplement the existing modes of demand response. The technical and economical feasibility of incorporating EV aggregator as a resource to the network is addressed in Ref. [21]. A conceptual regulatory framework and a business model to integrate EVs in the network and in turn support the power system operation is proposed in Ref. [22]. In Ref. [23], the authors propose an aggregated EV charging schedule in coordination with the SO. It is claimed that such charging schedules will enhance the grid efficiency and security, and thus allow significant EV penetration without a need for grid capacity expansion. Optimal and risk averse bidding strategies for EV aggregators under the constraints of market uncertainty, EV owners' behavior, and aggregators' profit volatility are presented in Refs. [24–26]. In Ref. [27], a stochastic programming methodology is developed with an objective of maximizing aggregator profit by charging the EVs on low price periods under time-varying market prices. They show that if the uncertainty in the number of vehicles in the parking lots is ignored, the aggregator profit is overestimated by 23.8%. A stochastic model from the SO's perspective in Ref. [28] incorporates demand response offered by the EVs. The model shows that SO can minimize the operation cost by optimally scheduling conventional generators, and the aggregators can minimize the electricity payment through DR participation. The objective of minimizing the cost of EV parking lot operation was approached via a cooperative game model in Ref. [29] and a non-cooperative game model in Ref. [30]. The cooperative game model reduced the cost through negotiation with the utility and the non-cooperative model used a price-driven EV charging model. A decentralized pricing scheme is proposed in Ref. [31], where SO sends the price and quantity information to the load aggregator, and both parties iteratively reoptimize the system dispatch and EV charging. A bilevel model is proposed in Ref. [32] that captures the interactions between the SO and parking lots. The model determines the scheduled energy for the parking lots based on the price offered by SO. Results show that the SO could achieve a considerable reduction of 8–9% of its total daily operation cost through parking lots' participation in the reserve market. In another bilevel model [33], the interaction between an EV aggregator and a parking lot owner is examined.

We make two key observations from the literature reviewed above. First, pure dynamic pricing has long been recommended as an enabler for demand response. Many pilot projects in the U.S. and Europe have demonstrated the expected benefits of pure form of dynamic pricing. However, there is a gap in the literature for model-based support on how to develop strategies for dynamic pricing for different network structure and composition. The second observation is that though models for various aspects of EVs have been presented to the literature, to our knowledge, a model for EV integration under dynamic pricing has not yet been made openly available. Our paper addresses both of the observations.

The remaining paper is organized as follows. Section 2 describes the modeling approach. The two-layer model is presented in

Section 3. In Section 4, the model is implemented on a sample 5-bus PJM network with actual load data from PJM zones. Performance comparison of dynamic pricing and demand response strategies with other existing and adhoc policies is also given in Section 4. Concluding remarks are contained in Section 5.

2. Modeling approach

Our two-layer modeling approach is depicted in Fig. 1. Before discussing the model elements, we state some of the modeling considerations and limitations. The financial settlement occurs in two stages: in the DA and the RT markets. The SO determines the dynamic prices by considering the possible outcomes of both markets. Strategic aggregators manage the loads in the network that include fixed residential and business loads, and schedulable EV loads in large parking lots. These parking lots host a variety of vehicles with different battery types at different times of the day and for different periods of stay. EVs arrive and depart with different charge levels. Depending on the hourly price variation, the aggregators develop their demand response strategies by optimally deciding charging schedules for the EVs. We assume the time interval to be an hour. One limitation of our model is that the aggregators neither inject power back from the vehicles to the grid (V2G) nor engage in any other forms of temporal arbitrage for peer-to-peer trading. Under present electricity pricing policies and some of the prevailing battery technologies (e.g., lead-acid, NiMH), V2G operation is still considered not cost effective [34]. However, evolving battery technologies, like lithium ion, can withstand charge cycling and support V2G.

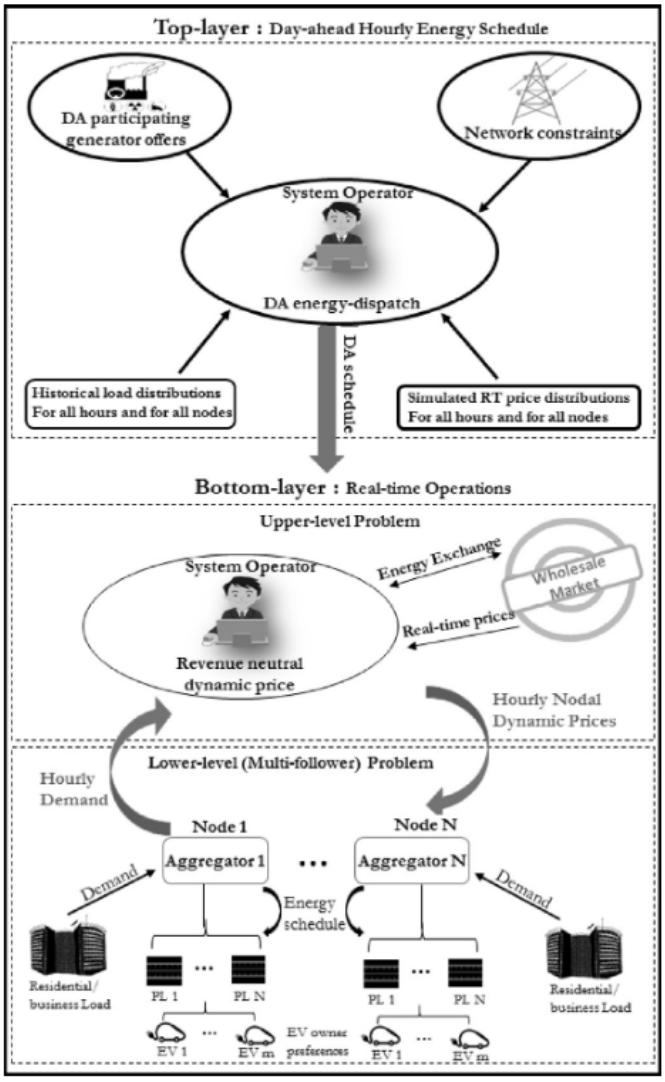

Fig. 1. Model components and their interactions.

The top-layer determines the DA quantities and prices for all hours of the day using DA generators' supply bids, historical demand patterns, and the corresponding RT prices. The model uses a network constrained least-cost dispatch principle for market clearing and is formulated as a two-stage stochastic program. The first stage determines the energy procured in the DA market, and the second stage decides the RT quantities. The RT prices are subjected to price spikes and are considered exogenous. The solution of the two-stage program yields scheduled DA hourly quantities and locational marginal prices (LMPs). These DA quantity-price pairs are sent to the bottom-layer model as input.

The bottom-layer is a bilevel model and is solved at the beginning of every hour. In the upper-level, the SO determines the dynamic prices for the hour using the lower-level problem as constraint. It minimizes the total cost of satisfying demands for the current and the future hours of the day, while meeting the key constraint of SO being revenue neutral. The RT prices are assumed to be known for the current hour, while the future hour RT prices are considered unknown and are modeled as uncertainty sets using a robust approach. The lower-level represents multiple aggregators (one for each load node) and obtains the optimal demand response actions. This is achieved by considering dynamic prices for the current hour and the DA prices as the estimates for the future hours. In what follows, we present a general framework for the two-layer model before presenting the complete model in the next section.

For the top-layer model, let c^N denote the supply offer of the generators and λ_ω^N denote the real-time prices for demand scenario ω. The decision variables for the energy procured in the DA and RT markets are denoted by E^{DA} and E_ω^{RT}, respectively. The probability distribution of each demand scenario is denoted by π_ω. The first constraint represents the first stage DA market operation and considers power balance, generator output, and transmission line limits. The dual variable (DA price) corresponding to the first stage constraint is denoted by λ^{DA}. The second constraint ensures the power balance in the RT market for all realizations ω of demand. The solution of the top-layer denoted by $\widehat{E}^{DA}$ and $\widehat{\lambda}^{DA}$ are sent to the bottom-layer. For simplicity, the index for time intervals of the day is omitted from the general formulation.

$$\text{Top}-\text{layer}\begin{cases}\min\limits_{E^{DA},E_\omega^{RT}} c^N E^{DA}+\sum\limits_{\omega\in\Omega}\pi_\omega\lambda_\omega^N E_\omega^{RT}, & \\ \text{s.t.} & \\ A^T E^{DA}\geq b, & \left(\lambda^{DA}\right)\\ p_\omega E^{DA}+q_\omega E_\omega^{RT}\geq\xi_\omega, & \forall\omega\in\Omega\\ E^{DA}\geq 0, E_\omega^{RT}\geq 0. & \forall\omega\in\Omega\end{cases}\tag{1}$$

$$\text{Bottom}-\text{layer}\begin{cases}\min\limits_{x\in X} F\left(x,y_1,\cdots,y_k\middle|\widehat{E}^{DA},\widehat{\lambda}^{DA}\right), & \\ \text{s.t.} & \\ G\left(x,y_1,\cdots,y_k\middle|\widehat{E}^{DA},\widehat{\lambda}^{DA}\right)\leq 0, & \\ y_i=\operatorname{argmin} f_i\left(x_i,y_i\middle|\widehat{\lambda}^{DA}\right), & \forall i=1,\cdots,k\\ g_i(x_i,y_i)\leq 0. & \forall i=1,\cdots,k\end{cases}\tag{2}$$

In the bottom-layer model, $x\in\mathbb{R}^k$ and $y_i\in\mathbb{R}$ are the decision

variables representing hourly dynamic prices (upper-level) and each aggregator's consumption (lower-level), respectively, where k denotes the number of aggregators (followers) in the network. The SO's objective function in the upper level, $F:\mathbb{R}^{2k}\rightarrow\mathbb{R}$, is to optimally procure energy in DA and RT markets. The objective function of the i^{th} aggregator at the lower level, $f_i:\mathbb{R}^2\rightarrow\mathbb{R}$, aims to minimize the total cost of energy consumption for the given dynamic price x_i. The upper and lower level constraints are denoted as $G(\cdot)$ and $g_i(\cdot)$, respectively.

The uniqueness of the above bilevel model is that it has multiple followers at the lower-level, and each follower's decision variable and the associated strategy space are independent of those of the other followers. The bilevel model can be reformulated as a single level MPEC as in Refs. [35,36] and are used in our solution approach. The lower-level model is linear and convex, and is reformulated as Karush-Kuhn-Tucker (KKT) optimality conditions (referred to as mathematical program with equilibrium constraint, MPEC). Big-M method and strong duality principle are used to linearize the model and thus obtain the equivalent single level MILP optimization model that can be solved using conventional approaches.

3. The model

In this section we present the details of the top and bottom-layer optimization models. As stated earlier, the top-layer is a two-stage stochastic model, and the bottom-layer is a bilevel robust optimization model.

3.1. Top-layer model

The top-layer concerns the DA market, where the SO decides the optimal DA scheduled quantities. The SO considers historical scenarios of demand patterns and corresponding RT prices at each node, together with the generator DA bids to determine the optimal DA schedule quantities. This is accomplished via a two-stage stochastic model where the first stage decides the DA quantities and the second stage obtains the RT quantities for all possible scenarios. The objective function minimizes the total expected cost of energy purchased in the DA and RT markets for all load nodes ($N_L\subset N$) and for all hours T. The term $C_g^{DA}(\cdot)$ denotes the cost function of participating generator $g\in N_G$ in the DA market. The decision variable for the generator output in the DA market is denoted by P_{gt}. The additional quantities purchased in the RT market in demand scenario ω (with probability π_ω) is denoted by $P_{gt}^{\omega,\Delta+}$. If the DA quantity exceeds demand in scenario ω, then the excess amount, denoted by $P_{gt}^{\omega,\Delta-}$, is assumed to be sold in the RT market. The RT price at node n and time t under demand scenario ω is denoted by $\lambda_{nt}^{RT,\omega}$.

Constraint (3) ensures the first stage network power balance. Let N_G^n denote the subset of the generators that are at node n, and B_n denote the set of nodes in the network that are directly connected to node n. For $m\in B_n$, let b_{nm} denote the susceptance of the line between the nodes n and m, and δ_{nt} denote the voltage angle (in radians) at node n and time t. The term E_{nt}^{DA} represents the scheduled DA quantity for the load node n and time t. Constraints (4) and (5) represent transmission line flow limits and generator output limits, respectively; $\overline{F}_{nm}$ represents the maximum line flow in MW, and $\underline{P}_g$ ($\overline{P}_g$) are lower (upper) limit of generator real power output in MW. Constraint (6) is used to designate node 1 as a reference bus (or slack bus) in the network. Constraint (7) ensures all other node buses are within the voltage angle limits.

$$\min\sum_{t=1}^{T}\left[\sum_{g\in N_G}C_g^{DA}(P_{gt})+\sum_{\omega\in\Omega}\pi_\omega\sum_{n\in N}\left\{\lambda_{nt}^{RT,\omega}\sum_{g\in N_G^n}\left(P_{gt}^{\omega,\Delta+}-P_{gt}^{\omega,\Delta-}\right)\right\}\right]$$

s.t.

First stage constraints

$$\sum_{g\in N_G^n}P_{gt}+\sum_{m\in B_n}b_{nm}[\delta_{nt}-\delta_{mt}]-E_{nt}^{DA}=0,\quad \forall n\in N,\forall t\in T \tag{3}$$

$$-\overline{F}_{nm}\le b_{nm}[\delta_{nt}-\delta_{mt}]\le\overline{F}_{nm},\quad \forall m\in B_n: m<n,\forall n\in N,\forall t\in T \tag{4}$$

$$\underline{P}_g\le P_{gt}\le\overline{P}_g,\quad \forall g\in N_G,\forall t\in T \tag{5}$$

$$\delta_{1t}=0,\quad \forall t\in T \tag{6}$$

$$-\pi\le\delta_{nt}\le\pi,\quad \forall n\in N,\forall t\in T \tag{7}$$

Second stage constraints

$$\sum_{g\in N_G^n}\left(P_{gt}^{\omega,\Delta+}-P_{gt}^{\omega,\Delta-}\right)+\sum_{m\in B_n}b_{nm}\left[\delta_{nt}^{\omega}-\delta_{mt}^{\omega}-\delta_{nt}+\delta_{mt}\right]-\left(E_{nt}^{RT,\omega,\Delta^+}-E_{nt}^{RT,\omega,\Delta^-}\right)=0,\quad \forall n\in N,\forall\omega\in\Omega,\forall t\in T \tag{8}$$

$$-\overline{F}_{nm}\le b_{nm}\left[\delta_{nt}^{\omega}-\delta_{mt}^{\omega}\right]\le\overline{F}_{nm},\quad \forall m\in B_n: m<n,\forall n\in N,\forall\omega\in\Omega,\forall t\in T \tag{9}$$

$$\underline{P}_g\le P_{gt}+P_{gt}^{\omega,\Delta+}-P_{gt}^{\omega,\Delta-}\le\overline{P}_g,\quad \forall g\in N_G,\forall\omega\in\Omega,\forall t\in T \tag{10}$$

$$E_{nt}^{DA}+E_{nt}^{RT,\omega,\Delta^+}-E_{nt}^{RT,\omega,\Delta^-}=D_{nt}^{\omega},\quad \forall n\in N_L,\forall\omega\in\Omega,\forall t\in T \tag{11}$$

$$E_{nt}^{DA}\ge\min_{\omega\in\Omega}D_{nt}^{\omega},\quad \forall n\in N_L,\forall t\in T \tag{12}$$

$$E_{nt}^{DA}\le\max_{\omega\in\Omega}D_{nt}^{\omega},\quad \forall n\in N_L,\forall t\in T \tag{13}$$

$$\delta_{1t}^{\omega}=0,\quad \forall\omega\in\Omega,\forall t\in T \tag{14}$$

$$-\pi\le\delta_{nt}^{\omega}\le\pi,\quad \forall n\in N,\forall\omega\in\Omega,\forall t\in T \tag{15}$$

$$P_{gt},P_{gt}^{\omega,\Delta+},P_{gt}^{\omega,\Delta-},E_{nt}^{DA},E_{nt}^{RT,\omega,\Delta^+},E_{nt}^{RT,\omega,\Delta^-}\ge 0$$

The remaining constraints are for the second stage model. Power balance for all RT demand realizations is ensured by constraint (8), where $E_{nt}^{RT,\omega,\Delta^+}$ and $E_{nt}^{RT,\omega,\Delta^-}$ are positive and negative demand deviations from the DA scheduled quantities. Constraint (9) and (10) are line flow and generator limits for all demand realizations. Constraint (11) ensures that total energy scheduled in the DA and RT markets matches the realized demand D_{nt}^{ω}. To ensure stable load scheduling, we have added constraints (12) and (13) such that the energy scheduled in the DA market is within the bounds of the realized demand. Constraints (14) and (15) represent the power angles for reference node and all other nodes, respectively. The dual variables of first stage constraints (3)-(5) can be decomposed into

marginal cost of energy at reference bus, marginal cost of power network losses, and cost of congestion, respectively. Using these dual values, the DA LMPs (denotes as λ_{nt}^{DA}) for all nodes and for all time periods are calculated. These LMPs and their associated quantities (E_{nt}^{DA}) are used as inputs in the bottom-layer model. Before presenting the bottom-layer model, we discuss how the RT prices ($\lambda_{nt}^{RT,\omega}$) are modeled using the approach in Ref. [37].

For each scenario ω, we solve the DCOPF model to get the market clearing prices (MCPs) at all nodes. We then express the RT prices as $\lambda_{nt}^{RT,\omega} = MCP_{nt}^{\omega}[1+\varepsilon]$, where $\varepsilon = M_1\varepsilon_1 + M_2\varepsilon_2$, and ε_1 and ε_2 are random variables, values of which are drawn from normal and Cauchy distributions with parameters (μ_1, σ_1) and (μ_2, σ_2), respectively; (M_1, M_2) is a bivariate random variable that takes values of (0,1) with probability p_s and (1,0) with probability $(1-p_s)$, where p_s is the probability of occurrence of price spikes. The normal random variable ε_1 contributes to the usual variability in the RT prices during off-peak periods, whereas the Cauchy random variable ε_2, chosen with probability p_s, generates the price spikes. Note that, the term ε and their related terms are also depend on node n and time t. For notation simplicity, the indexes are dropped.

3.2. Bottom-layer model

The bottom-layer is formulated as a bilevel model that is solved at the beginning of every hour. At the upper level, the SO determine appropriate dynamic prices at each load node for each hour, and at the lower level, the aggregators determine optimal consumption levels.

3.2.1. Upper-level model

The SO's goal in the model presented below is two-fold: 1) to minimize the total cost of satisfying the demand in the current and all future hours of the day, and 2) to ensure that the dynamic prices for the current hour are selected such that there is no significant revenue loss or surplus. Recall that the aggregators pay binding dynamic prices for the current hour, which may be different from the DA or RT prices. A robust approach is used to assess future RT prices.

$$\min \sum_{n\in N_L}\Bigg[\lambda_{n\tau}^{DA}E_{n\tau}^{DA} + \lambda_{n\tau}^{RT}\left(E_{n\tau} - E_{n\tau}^{DA}\right) + \sum_{t>\tau}^{T}\Bigg(\lambda_{nt}^{DA}E_{nt}^{DA} + \frac{1}{2}\left(\bar{\lambda}_{nt}^{RT} + \underline{\lambda}_{nt}^{RT}\right)\left(E_{nt} - E_{nt}^{DA}\right)\Bigg) + \Gamma_n^{RT}Z_n^{RT} + \sum_{t>\tau}^{T}\eta_{nt}^{RT}\Bigg],$$

s.t.

$$\pi_{n\tau}E_{n\tau} - \lambda_{n\tau}^{DA}E_{n\tau}^{DA} - \lambda_{n\tau}^{RT}\left(E_{n\tau} - E_{n\tau}^{DA}\right) \geq 0, \qquad \forall n\in N_L \tag{16}$$

$$Z_n^{RT} + \eta_{nt}^{RT} \geq \frac{1}{2}\left(\bar{\lambda}_{nt}^{RT} - \underline{\lambda}_{nt}^{RT}\right)y_{nt}, \qquad \forall n\in N_L, \forall t>\tau \tag{17}$$

$$-y_{nt} \leq \left(E_{nt} - E_{nt}^{DA}\right) \leq y_{nt}, \qquad \forall n\in N_L, \forall t>\tau \tag{18}$$

$$\pi_{n\tau}, Z_n^{RT}, \eta_{nt}^{RT}, y_{nt} \geq 0.$$

The objective function has two parts, cost of the current hour τ and the cost of all future hours $t>\tau$. For all load nodes (N_L), the first part accounts for the current hour cost of energy purchased in the DA and RT markets, where the RT price $\lambda_{n\tau}^{RT} = \lambda_{n\tau}^{DA}[1+\varepsilon]$ is the known for the current hour and $E_{n\tau}$ is the actual consumption level (decided at the lower-level model).

For the future hours ($t>\tau$), since the RT prices are uncertain, the cost is assessed via a robust model similar to that presented in Refs. [38,39]. Let $\left[\bar{\lambda}_{nt}^{RT}, \underline{\lambda}_{nt}^{RT}\right]$ denote the RT price confidence bounds, which are obtained from simulated sample values drawn from $\lambda_{nt}^{DA}[1+\varepsilon]$. Using a robust parameters Γ_n^{RT}, the SO minimizes the worst-case total cost. The parameter Γ_n^{RT} can take any value within the interval $[0, |T-\tau|]$. When it is 0, then the risk of RT price uncertainty is ignored in all future hours, and hence the RT prices are taken as the mean values of the confidence bounds. When $\Gamma_n^{RT} = \left|T-\tau\right|$, in all future hours most conservative decisions are considered, the RT prices are taken as: the upper bounds when additional quantities are purchased in the RT market, and the lower bounds when the DA quantities are sold in the RT market. The terms Z_n^{RT} and η_{nt}^{RT} are the robust model decision variables. The constraint (16) determines the dynamic prices $\pi_{n\tau}$ for the current hour τ such that there is no revenue shortfall/surplus for the SO. Constraint (17) and (18) are from the strong duality theory of robust optimization model.

3.2.2. Lower-level model

This model is used by each aggregator (one for each load node $n\in N_L$) to optimally plan consumption among the current and the remaining hours of a day. It uses the binding dynamic prices for the current hour, decided at the upper level model. For the remaining hours, the model uses the DA prices as estimates of dynamic prices. As noted earlier, only the parking lot portion of the total load is scheduled by the aggregator. Each parking lot is considered to host a large number of EVs, that flow in and out at different hours of the day, and have different charging needs.

$$\min \pi_{n\tau}E_{n\tau} + \sum_{t=\tau+1}^{T}\lambda_{nt}^{DA}E_{nt}$$

s.t.

$$E_{nt} = P_{nt}^{r}\Delta t + \sum_{p=1}^{N_n^{pl}}P_{nt}^{p}\Delta t, \quad (\rho_{nt}) \qquad \forall t\geq\tau \tag{19}$$

$$0 \leq P_{nt}^{p} \leq \overline{P}_{nt}^{p}, \quad \left(\underline{\mu}_{nt}^{p}, \overline{\mu}_{nt}^{p}\right) \qquad \forall t\geq\tau, \forall p\in N_n^{pl} \tag{20}$$

$$0 \leq SOC_{nt}^{p} \leq \overline{SOC}_{nt}^{p}, \quad \left(\underline{\nu}_{nt}^{p}, \overline{\nu}_{nt}^{p}\right) \qquad \forall t\geq\tau, \forall p\in N_n^{pl} \tag{21}$$

$$SOC_{nt}^{p} = SOC_{n(t-1)}^{p} + \eta_n^{p}P_{nt}^{p}\Delta t + \sum_{k\in C_n^{p}}\alpha_{nk}^{p}Q_{nk}^{p}T_{ntk}^{p} - \sum_{k\in C_n^{p}}\beta_{nk}^{p}Q_{nk}^{p}\widehat{T}_{ntk}^{p}, \quad (\psi_{nt}^{p}) \qquad \forall t\geq\tau, p\in N_n^{pl} \tag{22}$$

$$SOC_{nt}^{p} \geq \sum_{h\leq t}\sum_{k\in C_n^{p}}\alpha_{nk}^{p}Q_{nk}^{p}T_{nhk}^{p} - \sum_{h\leq t}\sum_{k\in C_n^{p}}\alpha_{nk}^{p}Q_{nk}^{p}\widehat{T}_{nhk}^{p}, \quad (\gamma_{nt}^{p}) \qquad \forall t\geq\tau, p\in N_n^{pl} \tag{23}$$

$$E_{nt}, P_{nt}^{p}, SOC_{nt}^{p} \geq 0$$

The first term of the objective function denotes the energy

consumption schedule for the current interval, and the second term accounts for the remaining hours. The constraint (19) ensures that the total load consumed is the sum of power consumed by fixed residential and business loads (P^r_{nt}) and the parking lots (P^p_{nt}), managed by the aggregator at node n in the time interval Δt, where N^{pl}_n is the number of parking lots at node n. Constraint (20) represents the maximum charging capacity of a parking lot, and constraint (21) ensures that the aggregate state of charge of a parking lot at any time t is not higher than the total capacity of the EVs present in the parking lot; the term $\overline{SOC}^p_{nt}$ is computed as $\sum_{h\le t}\sum_{k\in C^p_n} Q^p_{nk} T^p_{nhk} - \sum_{h\le t}\sum_{k\in C^p_n} Q^p_{nk} \widehat{T}^p_{nhk}$, where C^p_n is the maximum number of EVs in parking lot p and at node n, Q^p_{nk} is the battery capacity of vehicle k, and T^p_{ntk} and $\widehat{T}^p_{ntk}$ are binary variables for the time of arrival and the time of departure of the k^{th} EV. For instance, T^p_{ntk} value is 1, if k^{th} EV arrived at time t and 0 otherwise. Constraint (22) represents the state of charge at any time t, which is equal to the sum of: state of charge in the previous period $(t-1)$, power drawn from the grid for the parking lot in the interval Δt, and total state of charge of the vehicles arrived at time t, minus the total charge of the vehicles departed at time t. The coefficients η^p_n, α^p_{nk} and β^p_{nk} denote the conversion efficiency, percentage of charge at the time of arrival and departure, respectively. Constraint (23) ensures that the state of charge of the parking lot at any time t is at least equal to the sum of the initial state of charge of all parked EVs in the parking lot. The decision variables of the aggregator in this model are E_{nt}, P^p_{nt} and SOC^p_{nt} for all $t \ge \tau$. The dual variables associated with the constraints are given within the parentheses. We next formulate the KKT condition for the model. See Appendix A for the details.

3.2.3. Linearization of the upper-level model

The upper-level model has a nonlinear term $\pi_{n\tau}E_{n\tau}$ in (16). This nonlinearity is overcome by applying the strong duality principle on the lower-level model (see Section 3.2.2) as follows,

$$\pi_{n\tau}E_{n\tau} + \sum_{t=\tau+1}^{T}\lambda^{DA}_{nt}E_{nt} = \sum_{t\ge\tau}\Bigg[P^r_{nt}\rho_{nt}\Delta t - \sum_{p=1}^{N^{pl}_n}\Bigg\{\overline{P}^p_{nt}\overline{\mu}^p_{nt} + \overline{SOC}^p_{nt}\overline{\nu}^p_{nt} - \Bigg(\sum_{k\in C^p_n}\alpha^p_{nk}Q^p_{nk}T^p_{ntk} - \sum_{k\in C^p_n}\beta^p_{nk}Q^p_{nk}\widehat{T}^p_{ntk}\Bigg)\psi^p_{nt} - \Bigg(\sum_{h\le t}\sum_{k\in C^p_n}\alpha^p_{nk}Q^p_{nk}T^p_{nhk} - \sum_{h\le t}\sum_{k\in C^p_n}\alpha^p_{nk}Q^p_{nk}\widehat{T}^p_{nhk}\Bigg)\gamma^p_{nt}\Bigg\}\Bigg] + SOC^p_{n(\tau-1)}\psi^p_{n\tau}. \tag{24}$$

Note from the above that, for the strong duality components corresponding to $\psi^p_{n\tau}$ (from (22) in Section 3.2.2), we have added an additional term $SOC^p_{n(\tau-1)}\psi^p_{n\tau}$ at the end of the equation. This is to account for the time $t=\tau$ when $SOC^p_{n(\tau-1)}$ will be a constant (which otherwise is a variable for all $t>\tau$). Also, at $\tau = 1$, $SOC^p_{n(\tau-1)}$ is zero.

3.2.4. The single level linear model

The following formulation represents the transformed bi-level model into a single-level linearized MPEC model, where constraint (16) is linearized using (24).

$$\min \sum_{n\in N_L}\Bigg[\lambda^{DA}_{n\tau}E^{DA}_{n\tau} + \lambda^{RT}_{n\tau}\left(E_{n\tau} - E^{DA}_{n\tau}\right) + \sum_{t>\tau}^{T}\Bigg(\lambda^{DA}_{nt}E^{DA}_{nt} + \frac{1}{2}\left(\overline{\lambda}^{RT}_{nt} + \underline{\lambda}^{RT}_{nt}\right)\left(E_{nt} - E^{DA}_{nt}\right)\Bigg) + \Gamma^{RT}_n Z^{RT}_n + \sum_{t>\tau}^{T}\eta^{RT}_t\Bigg]$$

s.t.

$$\sum_{t\ge\tau}\Bigg[P^r_{nt}\rho_{nt}\Delta t - \sum_{p=1}^{N^{pl}_n}\overline{P}^p_{nt}\overline{\mu}^p_{nt} + \overline{SOC}^p_{nt}\overline{\nu}^p_{nt} - \Bigg(\sum_{k\in C^p_n}\alpha^p_{nk}Q^p_{nk}T^p_{ntk} - \sum_{k\in C^p_n}\beta^p_{nk}Q^p_{nk}\widehat{T}^p_{ntk}\Bigg)\psi^p_{nt} - \Bigg(\sum_{h\le t}\sum_{k\in C^p_n}\alpha^p_{nk}Q^p_{nk}T^p_{nhk} - \sum_{h\le t}\sum_{k\in C^p_n}\alpha^p_{nk}Q^p_{nk}\widehat{T}^p_{nhk}\Bigg)\gamma^p_{nt}\Bigg\}\Bigg] + SOC^p_{n(\tau-1)}\psi^p_{n\tau} - \sum_{t=\tau+1}^{T}\lambda^{DA}_{nt}E_{nt} - \lambda^{DA}_{n\tau}E^{DA}_{n\tau} - \lambda^{RT}_{n\tau}\left(E_{n\tau} - E^{DA}_{n\tau}\right) \ge 0, \quad \forall n\in N_L \tag{25}$$

Constraints (17) - (23) and (A.1) - (A.10),

$$\pi_{n\tau}, Z^{RT}_n, \eta^{RT}_{nt}, y_{nt}, E_{nt}, P^p_{nt}, SOC^p_{nt}, \rho_{nt}, \underline{\mu}^p_{nt}, \overline{\mu}^p_{nt}, \underline{\nu}^p_{nt}, \overline{\nu}^p_{nt}, \gamma^p_{nt} \ge 0,$$

ψ^p_{nt} – free variable.

4. Numerical results

We constructed a modified PJM 5-bus network in which the two load nodes are managed by aggregators. The loads consist of residential and business loads as well as large EV parking lots. The residential and business loads are assumed fixed, and only the parking lot loads are managed for demand response. We first give the network parameters, and then discuss implementation of our model on the network. Thereafter, we present a comparison of the total cost of meeting demands for policies derived from our model with other existing practices. The numerical experiments are carried out using Julia with Gurobi 7.0.1 solver on an Intel core i7 processor with 16 GB RAM.

4.1. Modified PJM 5-bus network

The network comprises three generating nodes with three generators in each, two load nodes, and six transmission lines (Fig. 2). Generator cost functions are quadratic and are obtained from Ref. [37]. The maximum limit of each generator is considered to be 800 MW. Demand at the two load nodes are constructed using 100 days of actual historical hourly demand data from two of the PJM zones DAY and AE for the year 2017 [40]. For computational simplicity, we first reduce the 100 demand patterns of each node into a small set of (five) representative dominant patterns with corresponding probabilities using the technique in Ref. [41]. The demand patterns are depicted in Fig. 3. We then calculate the average hourly demand of these five patterns, and considered 90 (85)% of the average hourly loads as the fixed loads for node 2 (node 3) and the rest as the EV load. Each of these patterns is considered as a demand scenario (ω) in the top-layer model. In the absence of historical data, demand at nodes can be forecasted based on socio-economic factors using methods discussed in Ref. [42]. The line connecting nodes 1 and 5 is considered to have a limited transmission capacity of 300 MW. The line reactances are as marked on

Fig. 2.

Aggregators at nodes 2 and 3 are each considered to manage 100 identical EV parking lots with the following characteristics. Each has a capacity of 1000 cars, of which 300 can be charged simultaneously. Each parking space has a charging rate of 11.5 kW (240 V, 48 A) with conversion efficiency (η_{in}^{p}) of 95%. Composition of the EVs is considered to be 60% Tesla Model S, 30% Nissan Leaf, and 10% Chevy Volt with battery capacities of 70 kWh, 40 kWh, and 18.4 kWh, respectively. The EVs are considered to arrive at the parking lots all hours of the day, with higher rates in the morning hours. EVs are considered to stay parked for at least 5 h, and depart at higher rates in the evening hours. The departure times of the vehicle in the lot are assumed known. Fig. 4 depicts simulated arrival and departure patterns of EVs in node 2. Similar patterns are generated for node 3. EVs are assumed to arrive at the parking lots with 20–40% charge, and leave with full charge. Charging of EVs require reactive power, which can cause an under voltage problem in the network. Hence, we have supplemented our DCOPF model with a constraint on the maximum number of vehicles that can be charged simultaneously (as stated before) to keep the reactive power consumption within a desirable level.

Before presenting the numerical results, we provide a brief step-by-step methodology for implementation of our two-layer model.

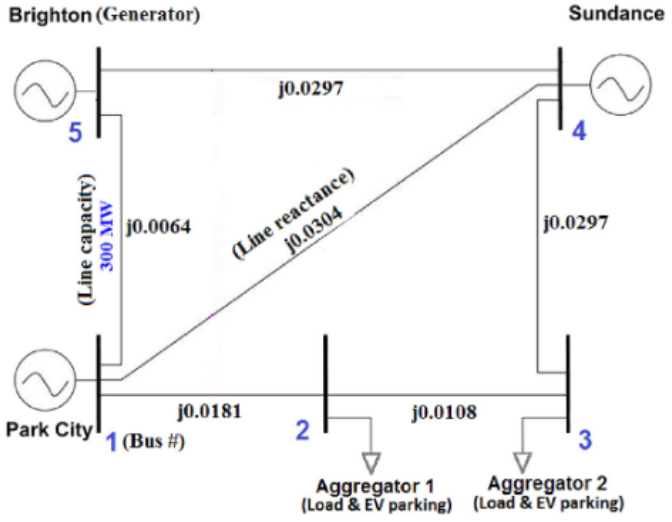

Fig. 2. Modified 5-bus PJM network.

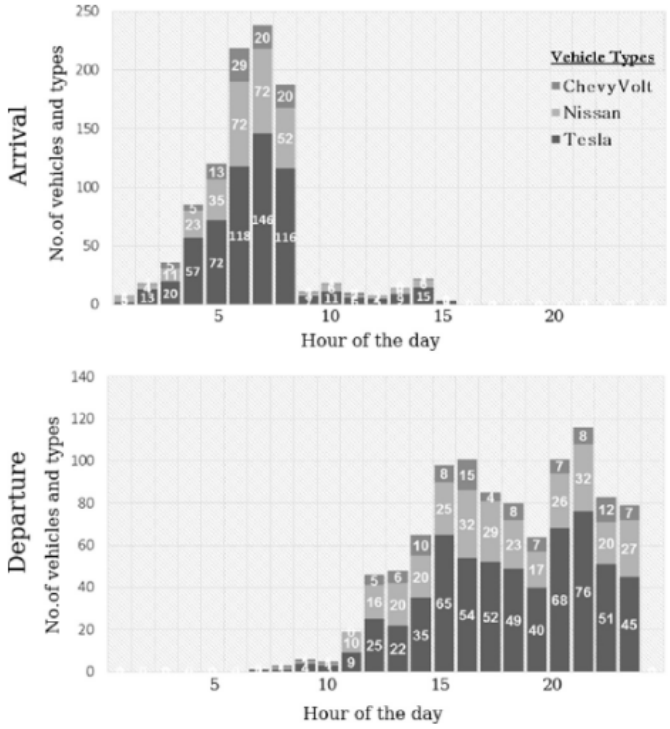

Fig. 4. Arrival and departure times of EVs of a parking lot at node 2.

- **Step 0:** The historical hourly demand data of each node is reduced to a set of dominant patterns (scenarios), product of which generates the total number of possible scenarios Ω. For each scenarios ($\omega \in \Omega$), we derive RT prices at each node and for all time periods. These demand patterns and corresponding RT prices serve as inputs for the top-layer model.
- **Step 1:** Using DA generators' supply bids, demand patterns and corresponding RT prices, the SO clears the DA market by solving the two-stage stochastic program that incorporates all network constraints. The solution of top-layer yields scheduled DA hourly quantities and corresponding DA prices, which are sent as input to the bottom layer.
- **Step 2:** The upper level of the bilevel model is solved by the SO to determine dynamic prices. The lower level model solves, for each aggregator, its energy consumption strategy. The bilevel model is reformulated as a single level MPEC model, which is further

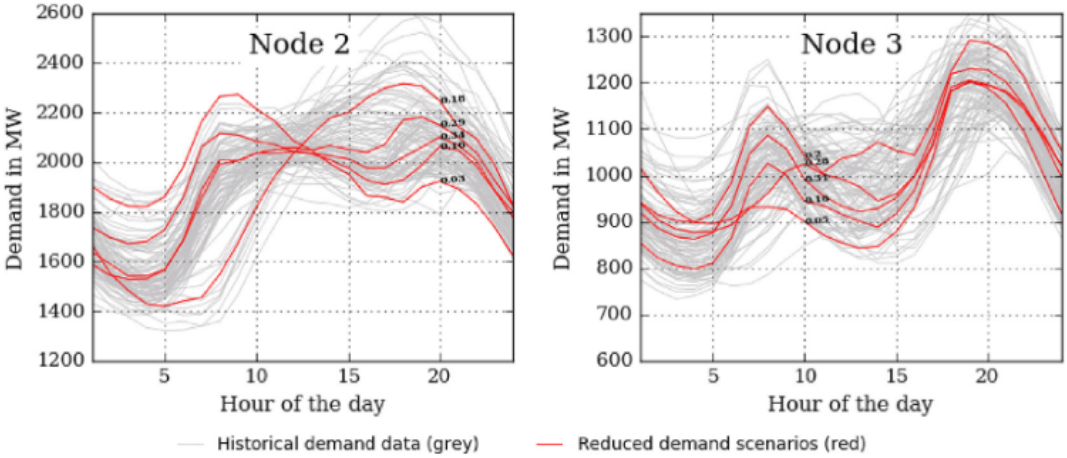

Fig. 3. Hourly demand scenarios for load at nodes 2 and 3.

linearized using strong duality principle. This converts the bilevel model into a single level MILP model.

4.2. Results from the top-layer model: DA market

The DA hourly quantities and prices for each load node are obtained from the two-stage stochastic program. For each demand scenario (ω) we derive RT prices, as discussed in Section 3.1. For which, the values for the parameters of the normal and Cauchy distributions are used as $(0, 0.1)$ and $(0.25, 0.05)$, respectively. The price spike probabilities (p_s) for different hours of the day at both load nodes are: $p_s = 0$ for hours 1–4 and 22–24; $p_s = 0.1$ for hours 5–12 and 19–21; $p_s = 0.25$ for hours 13–18. Note that, $p_s = k$ for an hour indicates that the RT price in that hour experiences spikes with a probability k.

Fig. 5 shows the DA quantities (in blue) in nodes 2 and 3 resulting from the top-layer two-stage stochastic model. The area shaded in grey represents the fixed residential and business loads, and the curves in red represent the demand scenarios. It may be observed that during the hours of no price spikes (e.g., hours 1–4 and 22–24), the DA scheduled quantities are close to the lowest demand scenario. This indicates that without the risk of price spikes, it is optimal to schedule less in DA market and procure any additional quantities during the actual hour in the RT market. On the other hand, when risk of price spike is higher the solution recommends higher DA quantities close to the highest demand scenario (e.g., hours 13–18). The numbers marked on the DA quantity curves in Fig. 5 are the hourly LMPs in $/MWh, which are sent as input to the bottom-layer model.

In this paragraph, using Fig. 6, we demonstrate how the RT price spikes can be adjusted in our model to represent various real scenarios. As shown in the box plots on top, for each value of p_s, from 0.1 to 0.9, we generated 30 samples of the RT prices considering a low value of the Cauchy distribution $\mu_2 = 0.25$ and MCP of $100/MWh. The box plots show the ratios of the RT price to MCP. Note that, for a low value of $p_s = 0.1$, the median of the ratio is close to one. The median rises to 1.3 for $p_s = 0.9$. The dots in the figure indicate the presence of sporadic larger spikes. This is similar to the average daily spikes encountered in ERCOT, NYSO, and CAISO markets. However, for higher values of the Cauchy distribution parameter μ_2, as shown in the bottom set of box plots, the price spike value increases, reaching to as high as six times higher than the MCP when $\mu_2 = 5.0$. Hence, by suitably selecting the parameters p_s and μ_2, our model can mimic price spike scenarios with different frequency of occurrence and magnitude.

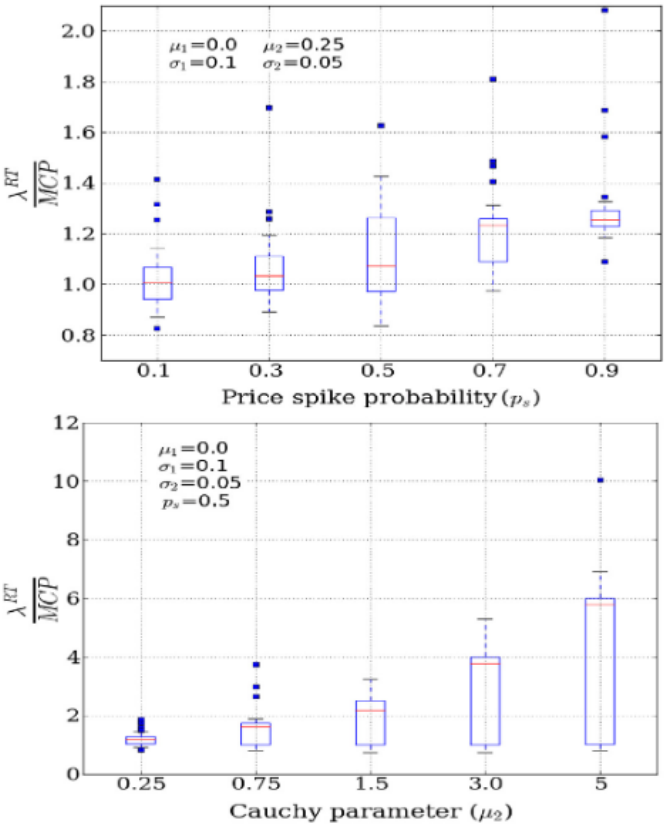

Fig. 6. RT price spikes for different p_s and μ_2.

4.3. Results from bottom-layer model: dynamic prices and EV charging schedules

Table 1 exhibits the bilevel model output for all 24 h for aggregator at node 2. These results are obtained using robust parameter (Γ_n^{RT}) value as 30%, and confidence bounds for future RT prices $\left[\underline{\lambda}_{nt}^{RT}, \overline{\lambda}_{nt}^{RT}\right]$ as 10% and 90%. We make several key observations from Table 1 using the rows in bold fonts.

It can be seen for hour 1 that the DA procured quantity is 1664.15 MW at a DA price of $93.3/MWh, while the actual total consumption is 1498.21 MW and the RT price of $113.53/MWh. As

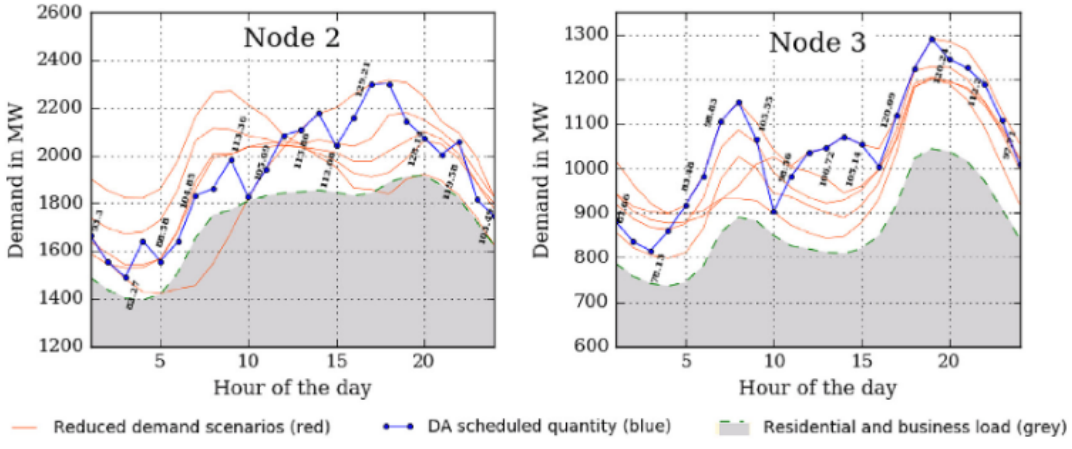

Fig. 5. DA scheduled quantities and corresponding prices at nodes 2 and 3.

Table 1
Load aggregator at node 2.

Time	DA Quantity (MW)	DA Price ($/MWh)	Dynamic price ($/MWh)	Total Demand (MW)	EV consumption (MW)	Resi. Demand (MW)	RT Price ($/MWh)	$\bar{\lambda}^{RT}$ ($/MWh)	$\underline{\lambda}^{RT}$ ($/MWh)	p_s
1	**1664.15**	**93.3**	**91.05**	**1498.21**	**9.2**	**1489.01**	**113.53**	**109.38**	**82.94**	**0**
2	1555.11	87.56	86.98	1466.16	29.9	1436.26	97.27	106.05	80.16	0
3	1490.51	82.27	82.3	1472.88	71.3	1401.58	79.92	104.08	78.66	0
4	**1642.6**	**91.99**	**92.28**	**1563.55**	**169.05**	**1394.5**	**86.4**	**105.22**	**78.69**	**0**
5	1557.34	88.58	88.58	1725.22	307.05	1418.18	88.58	110.28	76.67	0.1
6	1641.01	94.65	94.24	1855.67	345	1510.67	91.12	116.94	81.34	0.1
7	**1831.76**	**104.85**	**103.33**	**1999.39**	**345**	**1654.39**	**86.78**	**130.54**	**87.62**	**0.1**
8	**1862.7**	**107.39**	**106.66**	**1750.75**	**0**	**1750.75**	**118.78**	**135.44**	**90.74**	**0.1**
9	1985.29	113.36	113.36	2095.62	321.81	1773.81	113.36	131.04	94.09	0.1
10	1825.39	107.29	107.29	2154.85	345	1809.85	107.29	134.72	95.2	0.1
11	1943	105.09	105.72	2174.77	345	1829.77	111.04	130.23	95.96	0.1
12	2086	112.55	112.55	2059.56	216.98	1842.58	112.52	130.17	96.06	0.1
13	2106.64	113.86	113.62	2192.86	345	1847.86	107.75	140.77	97	0.25
14	2177	116.65	115.07	1855.25	0	1855.25	125.74	137.67	96.52	0.25
15	2041.95	112.08	107.64	1845.2	0	1845.2	153.72	139.43	95.4	0.25
16	2157.47	116.38	112.42	1830.31	0	1830.31	138.54	140.62	94.79	0.25
17	2299	129.21	129.18	1842.7	0	1842.7	129.32	142.88	97.36	0.25
18	2302.44	140.59	137.37	1887.11	0	1887.11	155.22	154.04	102.38	0.25
19	**2146.26**	**128.14**	**128.63**	**2242.1**	**331.33**	**1910.76**	**139.64**	**143.03**	**103.71**	**0.1**
20	2074.99	131	130.31	2261.82	345	1916.82	122.62	144.85	105.94	0.1
21	2005.33	119.58	117.44	2194.36	319.7	1874.66	94.79	138.48	103	0.1
22	2059.31	118.19	117.88	1991.72	171.84	1819.88	127.13	129.83	98.82	0
23	1817.92	103.49	103.48	1812.01	90.85	1721.16	106.47	123.09	93.68	0
24	1746.14	100.6	98.74	1621.47	0	1621.47	124.81	115.35	87.92	0

the RT price spike probability at this time is zero, the DA market schedules a quantity close to the lowest demand scenario. However, even without the spike, the basic variations in the RT price (modeled by normal distribution) has yielded a relatively high RT price of $113.53. As a result, the model chose to consume less than DA quantity and sell remaining in the RT market at a higher RT price. To balance this excess revenue, the revenue neutral SO offers a dynamic price ($91.05) that is lower than DA price ($93.3). Similar observations can be made for hour 8. Even with the presence of a significant number of EVs in the parking lots, optimal decision is not to charge any vehicles and keep the total demand low. At hour 4, the DA quantity is 1642.6 MW at a DA price of $91.99/MWh and RT price is $86.4/MWh. Though the RT price is lower, at hour 4, as the EV charging demand is low, the total demand is lower than the DA quantity. The excess DA amount is traded in the market at the RT price that is lower than DA price. To recover this loss, the revenue neutral SO selects a dynamic price that is higher than DA price. At hour 7, the DA quantity is 1831.76 MW at a DA price of $104.85/MW. The RT price $86.78/MWh is much lower than the DA price (as in hour 4). However, in contrast to hour 4, hour 7 has sufficient demand in the network to consume all of DA scheduled quantity and more. Hence, the SO offers a dynamic price ($103.33) that is lower than the DA price to promote consumption above the DA quantity. A final observation that we make is about time periods 8 and 19. At hour 8, the RT price is $118.78/MWh and the EV consumption is zero, whereas at hour 19, with RT price as $139.64/MWh and the EV consumption is very high (331.33 MW). This difference can be attributed to the vehicle charging needs close to departure times as well as the decisions the model made in previous hours 14–18 not to charge any EVs due to high RT prices.

For ease of further exposition of the numbers in Table 1, we develop combined plot of five of the columns from Table 1: DA price, RT price, lower and upper price bounds, and the total EV consumption (see Fig. 7). It depicts the trajectories of the DA and RT prices as well as the total hourly EV consumption. It may be noted that EV charging is avoided, when possible, during times of price spikes.

Results similar to those for node 2 are also observed for load at node 3. The daily average dynamic price for aggregators at nodes 2 and 3 are $109.45/MWh and $102.90/MWh, respectively. This difference can in part be attributed to the congestion in the network. Hereafter, we examine separately the impact of demand response and pricing practices on the daily cost to the consumers.

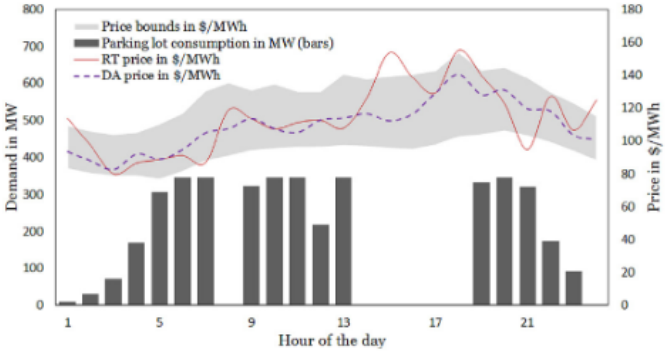

Fig. 7. Visualization of some results from Table 1.

4.4. Impact of demand response and pricing practice

Here, we first examine the impact of demand response via optimal charging of EVs on the network. This is done by comparing the total cost to consumers under optimal charging with the cost of an adhoc EV charging strategy with no demand response. Those costs are assessed under the same dynamic pricing policy of our model. The comparison is replicated four times. For the optimal charging strategy, the solution is obtained for three different values of the robust parameter Γ_n^{RT} (0, 0.3, and 0.5). The comparison results for load node 2 are presented in Table 2. In all four replicates, the total cost of meeting the demands under optimal EV charging strategy is lower than the adhoc strategy. Based on the average values shown in the last row, the overall average dynamic price with demand response is $1.4/MWh lower than that of dynamic price with no demand response (adhoc policy). Also, the total

Table 2
Optimal policy vs adhoc policy for load at node 2.

Optimal policy						Adhoc policy	
$\Gamma_n^{RT}=0$		$\Gamma_n^{RT}=0.3$		$\Gamma_n^{RT}=0.5$			
Total cost	Avg.DP ($/MWh)	Total cost	Avg.DP ($/MWh)	Total cost	Avg.DP ($/MWh)	Total cost	Avg.DP ($/MWh)
$4,996,992	110.08	$4,994,972	110.04	$5,007,262	110.31	$5,047,213	111.19
$4,961,292	109.30	$4,968,471	109.45	$4,987,796	109.88	$5,022,622	110.65
$4,966,925	109.42	$4,943,053	108.89	$4,941,478	108.86	$5,063,857	111.55
$5,156,280	113.59	$5,159,984	113.67	$5,167,509	113.84	$5,217,924	114.95
$5,020,372	**110.60**	**$5,016,620**	**110.51**	**$5,026,011**	**110.72**	**$5,087,904**	**112.08**

consumer cost saving from demand response is $70,000 per day. Similar results are observed for load node 3, which yield a reduction in the daily average dynamic price of $1.8/MWh and the daily cost saving of $45,000. Hence, the total consumer cost saving obtain via demand response for nodes 2 and 3 (with EV parking lots representing 10% and 15% of the total loads) for the sample 5-bus network is $115,000 per day and $42 million per year.

We now compare the benefits of our dynamic pricing strategy with those obtained from the commonly used pricing practices: flat pricing, TOU pricing, and CPP. We present the comparison for load node 3 (See Table 3). For the flat pricing policy, we consider the average of the 24 hourly DA prices at node 3 (from the top-layer model) as the fixed price throughout the day, which is obtained as $102.58/MWh. For TOU pricing, we assume that flat price of $102.58/MWh prevails for all hours except the peak hours 13–18 when the price is 1% higher ($103.61). For CPP, we consider the same flat price except for the hours when the RT price exceeds the flat price by 20%, at those times the price increases by 1%.

Table 3 exhibits the results for daily average price ($/MWh), cost to the consumers, and revenue of SO for all the above pricing practices. Also given within parenthesis (in bold) are the effective cost to the consumers for each pricing practice. The effective costs are used for fair comparison and are obtained by passing the SO's revenue shortfall/surplus to the consumers cost. The dynamic pricing policy, implemented with Γ_n^{RT} as 30%, results in a daily average price of $101.85/MWh (less than the flat price) with a total consumer cost of $2,529,117 and SO revenue of $21 (approximately revenue neutral). For flat pricing policy, the total daily effective cost to consumers is $36,584 higher than the dynamic pricing policy. The SO experiences a revenue loss of $18,388 in TOU. We examined two other adhoc flat pricing scenarios with prices 1% higher (row 2) and 1% lower (row 3) than the fixed price of $102.58/MWh. In the case of 1% higher price, which is motivated by the desire to avoid SO revenue loss, the effective cost to consumer remains the same while the SO revenue swings to a surplus of $7190. When flat price is reduced by 1%, the SO revenue loss soars to $43,716. For TOU pricing policy, the effective cost to consumers is higher by $10,897 than the dynamic policy. As in the case of flat pricing, we examine two other TOU scenarios with flat prices 1% higher and lower. For CPP, the effective cost to consumer is $2418 higher than the dynamic pricing. As in flat and TOU policies, outcomes for the two other CPP scenarios are not as desirable as the revenue neutral dynamic pricing policy. The effective cost to consumers decreases in the pricing sequence: flat, TOU, CPP and dynamic. Similar observations are also obtained for load node 2.

5. Concluding remarks

We have developed a robust game-theoretic model that simultaneously yields hourly binding dynamic prices of electricity (for SO) and the corresponding demand response actions using EVs (for load aggregators). The model aims to minimize the cost to consumers in a network subjected to price spikes, and keep the SO revenue neutral. Our model is formulated as a two-layer optimization model where the top-layer is a two-stage stochastic model and the bottom-layer is a bilevel model. We have demonstrated the implementation of the model on a modified 5-bus PJM network in which 10–15% of the total load is consumed by EVs that participate in DR; thermostatic loads are not considered as part of DR. A low to moderate price spike scenario where the median price is 1.25–1.5 times higher than the base price is examined. It is shown that by using dynamic pricing and demand response, the daily average consumer cost is 1.5% lower than the cost when dynamic pricing is offered but no demand response actions are taken. The consumer cost resulting from the use of our dynamic pricing and demand response policy is also compared with the cost from the flat pricing policy, for which we achieve a reduction of 1.42%. We also implemented our model on a high price spikes scenario with a median price spike 3.5 times higher than the base price. For this, we achieve a daily average consumer cost reduction of 6.5% from flat pricing. It is evident that our model is able to accommodate price spikes and yield appropriate policy for dynamic pricing and demand response to support SOs and load aggregators. The above mentioned benefits of our model are quite as expected, as researchers and practitioners have long predicted that a true form of dynamic pricing and network wide demand response will bring such benefits. A recent paper claimed the expected cost benefits to be between 2 and 4% [6].

Table 3
Comparison of dynamic pricing with traditional pricing for load at node 3.

Dynamic pricing			Flat Pricing			TOU pricing			CPP		
Avg $/MWh	Total cost ($)	SO Revenue ($)	Avg $/MWh	Total cost ($)	SO Revenue ($)	Avg $/MWh	Total cost ($)	SO Revenue ($)	Avg $/MWh	Total cost ($)	SO Revenue ($)
101.85	2,529,117 **(2,529,096)**	21	102.58	2,547,292 **(2,565,680)**	−18,388	102.58, 103.61	2,552,681 **(2,539,993)**	12,688	102.58, 103.61	2,551,021 **(2,531,514)**	19,508
			103.61	2,572,869	7190	103.61, 104.64	2,578,258	38,265	103.61, 104.64	2,576,599	46,818
			101.56	2,521,963	−43,716	101.56, 102.57	2,527,247	−12,746	101.56, 102.57	2,526,653	−3699

We note that, application of our model in real networks with many buses will introduce a number of computational challenges. For example, in the top-layer model the total number of demand scenarios (Ω) will increase exponentially with the number of load buses. The constraint matrix of the network, in the top-layer model, will also grow large and sparse. Use of efficient scenario reduction techniques (as in Ref. [41]) and inherent capability of Gurobi optimizer to deal with sparse matrices can be used to alleviate some of the above challenges. As far as the bottom layer model is concerned, the number of EV aggregator models that we need to solve in the lower level will increase linearly with the number of load buses. Since these models are considered to be independent of each other, a distributed computational approach can address this. Implementation of our model for a large network therefore is a topic of future research.

Appendix A. KKT formulation for the lower-level (aggregator's) model

In order to convert the bilevel model of the bottom-layer into a single level mixed integer programming model, we write the KKT conditions for each load node in the lower-level. The KKT conditions comprise the set of stationarity conditions (A.1)-(A.5) with respect to dual variables of the aggregator's problem, complementary slackness conditions (A.6)-(A.10), and collection of constraints (19)-(23). The KKT conditions for a load node $n \in N_L$ are given as follows.

$$\rho_{n\tau} \leq \pi_{n\tau}, \quad (E_{n\tau}) \tag{A.1}$$

$$\rho_{nt} \leq \lambda_{nt}^{DA}, \quad (E_{nt}) \qquad \forall t > \tau \tag{A.2}$$

$$-\rho_{nt}\Delta t + \underline{\mu}_{nt}^{p} - \overline{\mu}_{nt}^{p} - \eta_n^p \psi_{nt}^{p}\Delta t \leq 0, \quad (P_{nt}^{p}) \qquad \forall t \geq \tau, \forall p \in N_n^{pl} \tag{A.3}$$

$$\underline{\nu}_{nt}^{p} - \overline{\nu}_{nt}^{p} + \psi_{nt}^{p} - \psi_{n(t+1)}^{p} + \gamma_{nt}^{p} \leq 0, \quad (SOC_{nt}^{p}) \quad \forall t = \tau, \cdots, T-1, \forall p \in N_n^{pl} \tag{A.4}$$

$$\underline{\nu}_{nt}^{p} - \overline{\nu}_{nt}^{p} + \psi_{nt}^{p} + \gamma_{nt}^{p} \leq 0, \quad (SOC_{nt}^{p}) \qquad \forall t = T, \forall p \in N_n^{pl} \tag{A.5}$$

$$0 \leq \underline{\mu}_{nt}^{p} \perp P_{nt}^{p} \geq 0, \qquad \forall t \geq \tau, \forall p \in N_n^{pl} \tag{A.6}$$

$$0 \leq \overline{\mu}_{nt}^{p} \perp \left(\overline{P}_{nt}^{p} - P_{nt}^{p}\right) \geq 0, \qquad \forall t \geq \tau, \forall p \in N_n^{pl} \tag{A.7}$$

$$0 \leq \underline{\nu}_{nt}^{p} \perp SOC_{nt}^{p} \geq 0, \qquad \forall t \geq \tau, \forall p \in N_n^{pl} \tag{A.8}$$

$$0 \leq \overline{\nu}_{nt}^{p} \perp \left(\overline{SOC}_{nt}^{p} - SOC_{nt}^{p}\right) \geq 0, \forall t \geq \tau, \forall p \in N_n^{pl} \tag{A.9}$$

$$0 \leq \gamma_{nt}^{p} \perp \left[SOC_{nt}^{p} - \left(\sum_{h \leq t} \sum_{k \in C_n^p} \alpha_{nk}^{p} Q_{nk}^{p} T_{nhk}^{p} - \sum_{h \leq t} \sum_{k \in C_n^p} \alpha_{nk}^{p} Q_{nk}^{p} \widehat{T}_{nhk}^{p} \right) \right] \geq 0, \quad \forall t \geq \tau, \forall p \in N_n^{pl} \tag{A.10}$$

$$\rho_{nt}, \underline{\mu}_{nt}^{p}, \overline{\mu}_{nt}^{p}, \underline{\nu}_{nt}^{p}, \overline{\nu}_{nt}^{p}, \gamma_{nt}^{p} \geq 0, \psi_{nt}^{p} - \text{free variable}.$$

Note that, the stationarity condition for the primal variable (E_{nt}) is split into two parts, for the current hour τ (A.1) and for all future hours $t > \tau$ (A.2). Similarly, for the primal variable SOC_{nt}^{p}, we have two inequalities, one for all $t < T$ (A.4) and the other for T (A.5), as there is no state update from T to $T+1$. The complementary slackness conditions (A.6)-(A.10) are of the general form $0 \leq u \perp h(x) \geq 0$, which are linearized by substituting with the following: $u \geq 0$, $h(x) \geq 0$, $u \leq Mz$ and $h(x) \leq M(1-z)$, where (big) M is a large constant and z is a 0–1 binary decision variable.

References

[1] Borenstein S, Jaske M, Rosenfeld A. Dynamic pricing, advanced metering, and demand response in electricity markets. UC Berkeley: Center for the Study of Energy Markets; 2002.
[2] Dutta G, Mitra K. A literature review on dynamic pricing of electricity. J Oper Res Soc 2017;68(10):1131–45.
[3] Khan AR, Mahmood A, Safdar A, Khan ZA, Khan NA. Load forecasting, dynamic pricing and dsm in smart grid: a review. Renew Sustain Energy Rev 2016;54:1311–22.
[4] Hu Z, Kim J-h, Wang J, Byrne J. Review of dynamic pricing programs in the us and europe: status quo and policy recommendations. Renew Sustain Energy Rev 2015;42:743–51.
[5] Faruqui A, Hledik R, Newell S, Pfeifenberger H. The power of 5 percent. Electr J 2007;20(8):68–77.
[6] Faruqui A, Hajos A, Hledik R, Newell S. Fostering economic demand response in the Midwest ISO. Energy 2010;35(4):1544–52.
[7] LCG consulting, energy price, http://www.energyonline.com/, accessed: June, 12, 2018.
[8] Block D, Harrison J, Center FSE, Dunn MD. Electric vehicle sales and future projections, electric vehicle transportation center. University of Central Florida; 2014. Tech. Rep (1).
[9] Quillinan JD. Pricing for retail electricity. J Revenue Pricing Manag 2011;10(6):545–55.
[10] Kaluvala NS, Forman A. Smart grid. Int J E Polit 2013;4(2):39–47.
[11] Faruqui A, Sergici S, Akaba L. The impact of dynamic pricing on residential and small commercial and industrial usage: new experimental evidence from Connecticut. Energy J 2014:137–60.
[12] Faruqui A, Palmer J. The discovery of price responsiveness–a survey of experiments involving dynamic pricing of electricity. Brattle group; 2012.
[13] Ahmad F. The ethics of dynamic pricing. Electr J 2010;23:13–27.
[14] Borenstein S. Effective and equitable adoption of opt-in residential dynamic electricity pricing. Rev Ind Organ 2013;42(2):127–60.
[15] Ottesen SO, Tomasgard A, Fleten S-E. Prosumer bidding and scheduling in electricity markets. Energy 2016;94:828–43.
[16] Ottesen SO, Tomasgard A, Fleten S-E. Multi market bidding strategies for demand side flexibility aggregators in electricity markets. Energy 2018;149:120–34.
[17] Iria J, Soares F, Matos M. Optimal supply and demand bidding strategy for an aggregator of small prosumers. Appl Energy 2018;213:658–69.
[18] Gomez-Herrera JA, Anjos MF. Optimal collaborative demand-response planner for smart residential buildings. Energy 2018;161:370–80.
[19] Mohseni A, Mortazavi SS, Ghasemi A, Nahavandi A, et al. The application of household appliances' flexibility by set of sequential uninterruptible energy phases model in the day-ahead planning of a residential microgrid. Energy 2017;139:315–28.
[20] Subramanian V, Das TK, Kwon C, Gosavi A. Data-driven learning model for dynamic pricing and demand response in smart and connected communities. 2017. http://vigneshs.myweb.usf.edu/publications/index.html/. [Accessed 12 June 2018].
[21] Bessa RJ, Matos MA. Economic and technical management of an aggregation agent for electric vehicles: a literature survey. Int Trans Electr Energy Syst 2012;22(3):334–50.
[22] San Román TG, Momber I, Abbad MR, Miralles AS. Regulatory framework and business models for charging plug-in electric vehicles: infrastructure, agents, and commercial relationships. Energy Pol 2011;39(10):6360–75.
[23] Ortega-Vazquez MA, Bouffard F, Silva V. Electric vehicle aggregator/system operator coordination for charging scheduling and services procurement. IEEE Trans Power Syst 2013;28(2):1806–15.
[24] Vayá MG, Andersson G. Optimal bidding strategy of a plug-in electric vehicle aggregator in day-ahead electricity markets under uncertainty. IEEE Trans Power Syst 2015;30(5):2375–85.
[25] Shafie-Khah M, Heydarian-Forushani E, Golshan M, Siano P, Moghaddam M, Sheikh-El-Eslami M, Catalão J. Optimal trading of plug-in electric vehicle aggregation agents in a market environment for sustainability. Appl Energy 2016;162:601–12.
[26] Momber I, Siddiqui A, San Román TG, Söder L. Risk averse scheduling by a PEV aggregator under uncertainty. IEEE Trans Power Syst 2015;30(2):882–91.
[27] Alipour M, Mohammadi-Ivatloo B, Moradi-Dalvand M, Zare K. Stochastic scheduling of aggregators of plug-in electric vehicles for participation in energy and ancillary service markets. Energy 2017;118:1168–79.
[28] Nezamoddini N, Wang Y. Risk management and participation planning of electric vehicles in smart grids for demand response. Energy 2016;116:

836–50.
[29] Aghajani S, Kalantar M. A cooperative game theoretic analysis of electric vehicles parking lot in smart grid. Energy 2017;137:129–39.
[30] Li J, Li C, Xu Y, Dong Z, Wong K, Huang T. Noncooperative game-based distributed charging control for plug-in electric vehicles in distribution networks. IEEE Trans Ind Inf 2018;14:301–10.
[31] Xi X, Sioshansi R. Using price-based signals to control plug-in electric vehicle fleet charging. IEEE Trans Smart Grid 2014;5(3):1451–64.
[32] Aghajani S, Kalantar M. Operational scheduling of electric vehicles parking lot integrated with renewable generation based on bilevel programming approach. Energy 2017;139:422–32.
[33] Neyestani N, Damavandi MY, Shafie-Khah M, Bakirtzis AG, Catalão JP. Plug-in electric vehicles parking lot equilibria with energy and reserve markets. IEEE Trans Power Syst 2017;32(3):2001–16.
[34] Zhou C, Qian K, Allan M, Zhou W. Modeling of the cost of ev battery wear due to v2g application in power systems. IEEE Trans Energy Convers 2011;26(4):1041–50.
[35] Wang Q, Yang F, Wang S, Liu Y-H. Bilevel programs with multiple followers. Syst Sci Math Sci 2000;13.
[36] Dempe S, Dutta J. Is bilevel programming a special case of a mathematical program with complementarity constraints? Math Program 2012;131(1–2):37–48.
[37] Das D, Wollenberg BF. Risk assessment of generators bidding in day-ahead market. IEEE Trans Power Syst 2005;20(1):416–24.
[38] Bertsimas D, Sim M. Robust discrete optimization and network flows. Math Program 2003;98(1–3):49–71.
[39] Rahimiyan M, Baringo L. Strategic bidding for a virtual power plant in the day-ahead and real-time markets: a price-taker robust optimization approach. IEEE Trans Power Syst 2016;31(4):2676–87.
[40] ISO PJM, U.S., https://www.pjm.com/, accessed: June, 12, 2018.
[41] Growe-Kuska N, Heitsch H, Romisch W. Scenario reduction and scenario tree construction for power management problems. In: Power tech conference proceedings, vol. 3. IEEE Bologna; 2003. p. 7. IEEE, 2003.
[42] Kaboli SHA, Selvaraj J, Rahim N. Long-term electric energy consumption forecasting via artificial cooperative search algorithm. Energy 2016;115:857–71.